

Supplemental Materials

Molecular Biology of the Cell

Buck et al.

Supplemental Materials

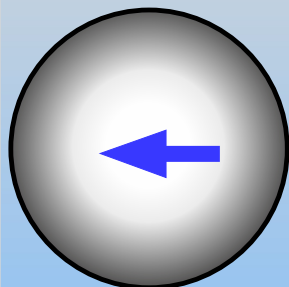
Supplemental Fig. 1. Flow calculation from 4E8 bead tracks. (A) Workflow for calculating retrograde flow maps. After initial tracking and smoothing of positions (white tracks), the user draws lines (shown in orange) to approximate flow direction (i), and selects points (white X's) to delineate the P-domain shape (ii). The MATLAB script fits two ellipses (ii) to define the leading edge (magenta) and end of P-domain (cyan) and subdivides the P-domain into an elliptical grid (iii) composed of four annular zones (see Fig. 5) and a variable number of sectors depending on the shape of the growth cone. The expected flow lines from (i) are used to calculate a smooth (interpolated) map of expected flow angles (iv). Then, local flow angles are subtracted from bead velocity angles to yield an angular velocity deviation map (v , detailed view corresponding to dashed black ROI outlined in i). Portions of bead tracks which exhibit angular velocity deviation $< 20^\circ$ and instantaneous velocity $< 9 \mu\text{m}/\text{min}$ are extracted to a new MATLAB variable for flow-only tracks (blue tracks in vi). The x and y positions and angular velocities θ of the flow data is convolved to create a coarse map of θ_{flow} (vii) which is then interpolated and masked for a pixel-level resolution map of θ_{flow} (viii). The elliptical grid generated in (iii) is used to calculate mean flow speed $|v_{flow}|$ in each box; these values are used to fit a locally weighted (lowess) surface (ix) which is then interpolated at pixel-level resolution and masked (x). Finally, the x and y flow velocity components, dx/dt_{flow} and dy/dt_{flow} , are calculated using trigonometry and mapped (xi, xiii); these maps are later used for subtracting local flow from observed bead X and Y velocities to yield $|v_{poly}|$ (see supplemental methods). (B) 4E8 beads were tracked (left panel) and retrograde flow was extracted and mapped (right panel, showing color-coded flow speeds and quiver plots of flow). *Scale bar*, 5 μm . *Inset*, magnified view of box outlined in white, showing intrapodia (arrow). (C) ConA beads applied to the same growth cone from (B) were tracked (left panel) and flow was mapped using the same approach (right panel). *Inset*, magnified view showing continued presence of intrapodia (arrow) despite absence of inductopodia.

Supplemental Figure 2. (A) Superimposed outlines of growth cone central domains (representative examples) at the end of control latencies (left), CK689 inactive analogue (center) or at the end of recordings in the presence of CK999 (right). Each color outline corresponds to the same growth cone in various conditions. (B) Superimposed outlines of growth cone central domains (representative examples) at the end of control latencies (left), or at the end of recordings in NSC23766 (right).

Supplemental Figure 3. Traced outlines of growth cone central domains at the end of evoked growth experiments. (A) Ten growth cones traced at the end of the advance period in control and inactive analog CK689, or at the end of recording in 50 μM CK666. (B) Ten growth cones traced at the end of advance period in control or at the end of recording in 100 μM NSC23766.

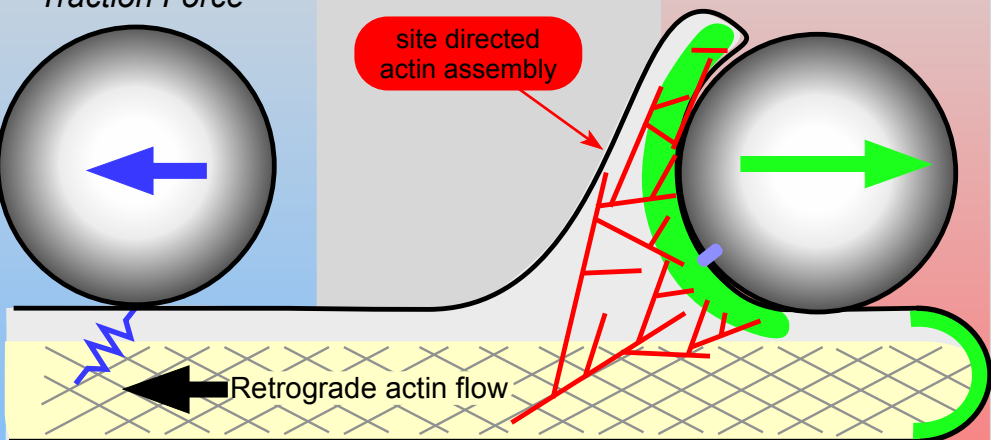
IgCAM coated bead behaviors in the peripheral domain of a neuronal growth cone

*Classical
Traction Force*



site directed
actin assembly

*Adhesion site propulsion
buffers traction force*



$$f_{poly} = 0$$

f_{flow}



$$f_{poly}$$

f_{flow}



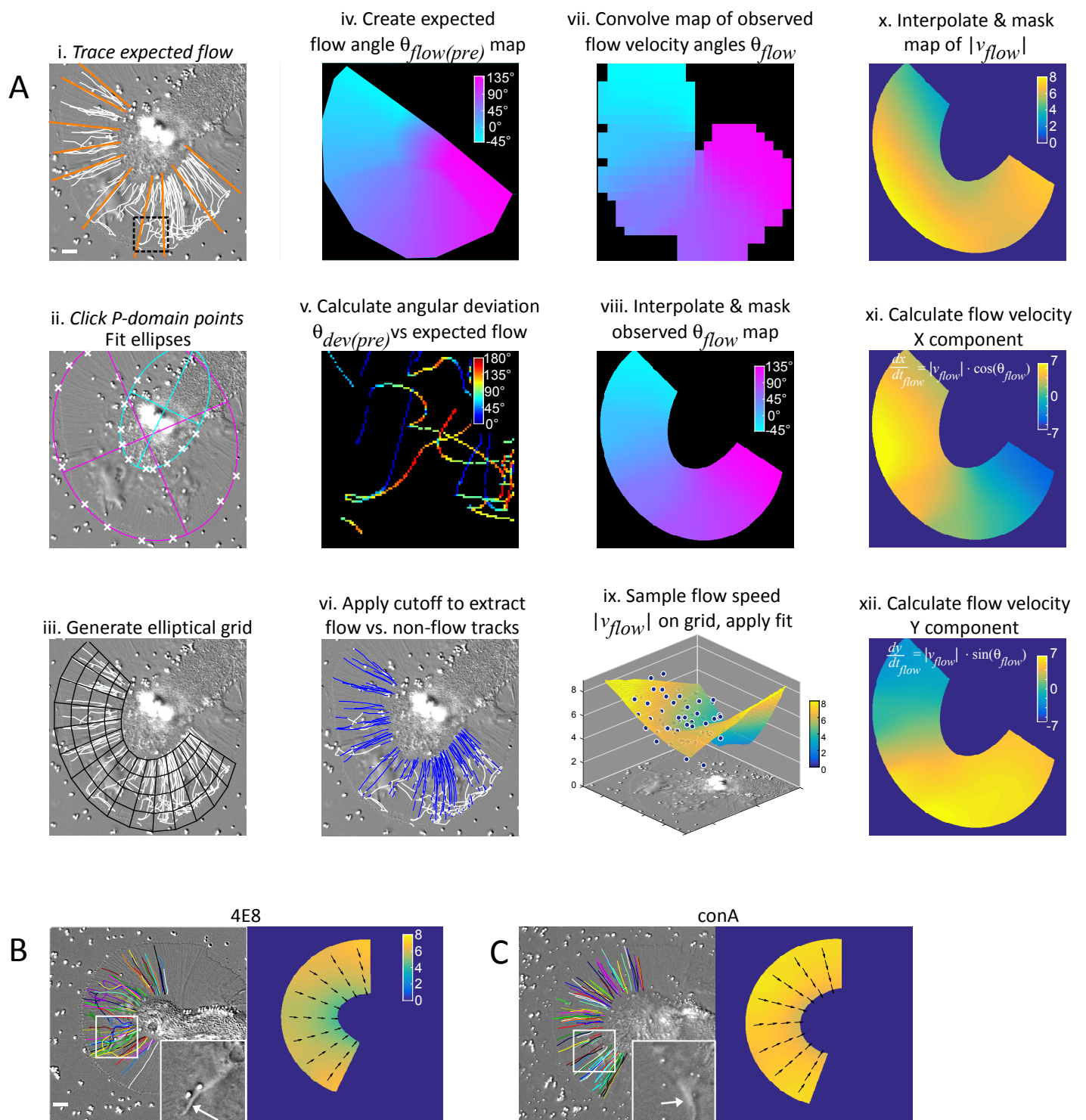


Figure S1

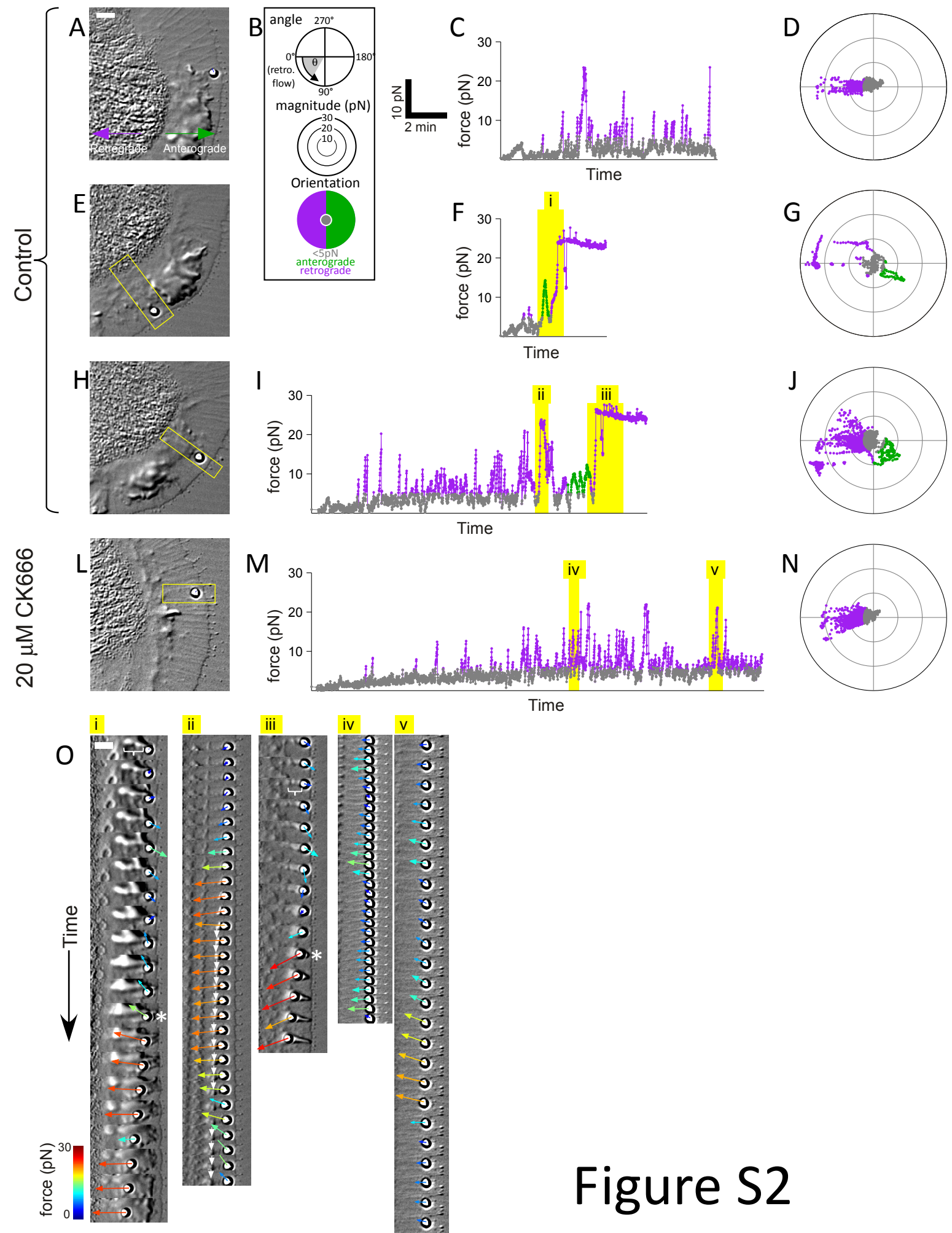


Figure S2

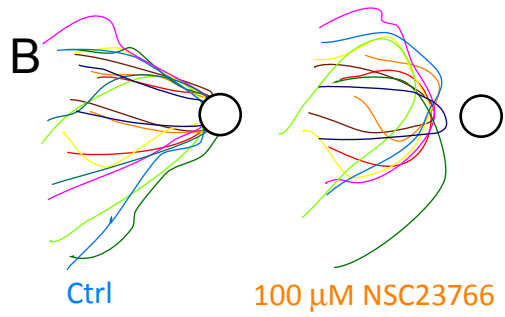
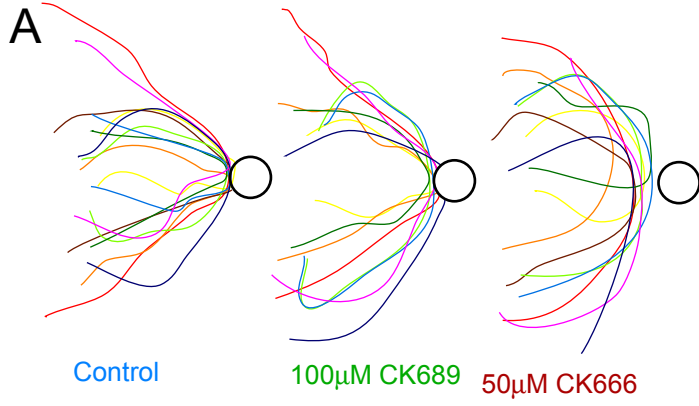


Figure S3